Heliyon 10 (2024) e33603

Contents lists available at ScienceDirect

Heliyon

journal homepage: www.cell.com/heliyon

Research article

Synthesis of silver nanoparticles assisted by aqueous root and leaf extracts of *Rhus chinensis* Mill and its antibacterial activity

Manisha Bhusal [a], Ishwor Pathak [b], Anita Bhadel [a], Deepak Kumar Shrestha [c], Khaga Raj Sharma [a,*]

[a] *Central Department of Chemistry, Tribhuvan University, Kirtipur, Kathmandu, Nepal*
[b] *Department of Chemistry, Amrit Campus, Tribhuvan University, Kathmandu, Nepal*
[c] *Department of Chemistry, Butwal Multiple Campus, Butwal, Nepal*

ARTICLE INFO

Keywords:
Antimicrobial activity
Green synthesis
Rhus chinensis
silver nanoparticles

ABSTRACT

In the present study, silver nanoparticles were synthesized using aqueous root and leaf extracts of *Rhus chinensis* Mill. This study aimed to undertake the green synthesis of silver nanoparticles utilizing plant extracts in an eco-friendly, cost-effective, and more efficient manner with its antibacterial application. The prepared silver nanoparticles (AgNPs) were characterized by using different techniques. Such as ultraviolet–visible spectroscopy (UV–Vis), Fourier transform infrared spectroscopy (FT-IR), x-ray diffraction spectroscopy (XRD), field emission-scanning electron microscopy (FE-SEM), and energy dispersive X-ray (EDX). The color changes from yellowish to reddish brown can be visualized and it indicates the formation of silver nanoparticles. The UV–Vis absorption peak shown by the synthesized AgNPs assisted by root and leaf extract was at 443 nm and 440 nm respectively. The functional group present in plants' secondary metabolites may act as capping and stabilizing agents, indicated by the shifting and disappearing of the peak in the plant extracts and the extracts-assisted synthetic nanoparticles. The crystallite size of synthesized AgNPs assisted by the root and leaf extracts of *Rhus cinensis* was found to be 11.01 nm and 13.39 nm respectively, while with the help of FE-SEM image the shape and particle size of synthesized AgNPs root and leaf extract was found spherical with particle diameter of 54.40 nm and 30.89 nm respectively. The presence of an intense silver component was confirmed by EDX analysis which showed an intense peak at around 3 Kev and other elements like Cl, O, C, and N were also reported in synthesized AgNPs. Both the plant extracts assisted synthesized AgNPs showed higher zones of inhibition (ZOI) against both the Gram-positive and Gram-negative bacteria. The results of the study indicate the potential benefit of synthesized silver nanoparticles using *Rhus chinensis* root and leaf extracts for biomedical purposes.

1. Introduction

Rhus chinensis (RC) is a tiny deciduous perennial shrub in which its leaves, roots, and fruit parts are used to cure depurative, costimulatory blood circulation, hemoptysis, inflammations, laryngitis, traumatic fractures, snake bite, colic, diarrhea, dysentery, jaundice, and hepatitis [1]. *Rhus chinensis* is a good traditional medicinal plant and is also rich in various biological activities that might

* Corresponding author.
E-mail address: khaga.sharma@cdc.tu.edu.np (K.R. Sharma).

https://doi.org/10.1016/j.heliyon.2024.e33603
Received 15 August 2023; Received in revised form 21 June 2024; Accepted 24 June 2024
Available online 27 June 2024

be used for HIV-1 infection chemotherapy, and RC-1 was efficient against HIV-1 [2]. Anticaries, antiosteoporosis, anti coronary heart disease, hepatoprotective, antiobesity, intestinal protection, gastroprotective, antidiabetic, antioxidation, anti-inflammatory, antibacterial, antiviral, anticancer, and other biological activities of *R. chinensis* have been reported which is used to cure various diseases.

Silver nanoparticles are nanoparticles of silver with sizes ranging from 1 nm to 100 nm [3]. Silver has been used by humans for around 7000 years, and throughout that time it has established a reputation as a very potent antibacterial agent that may destroy a variety of infectious diseases-causing germs [4]. Silver nanoparticles are being used more often in a wide range of sectors because of their unique physical and chemical properties. Comprising health care, pharmaceuticals, and consumer products. Biological characterization is among them powerful optical, electrical thermal, and conductivity characteristics [5]. Nowadays, silver nanoparticles (AgNPs) are widely used in a variety of fabrics, keyboards, bandages, and medical equipment. Due to the uniqueness of nanosized metallic particles, their ability to significantly alter physical and their ratio of surface to volume, and their chemical and biological capabilities these nanoparticles have been employed for several purposes [6]. The new generation of bio-nanoformulations is based on an integration of traditional medicine with nanotechnology [7].

These metal NPs have been prepared using many different methods. These include biological (plants, fungi, bacteria, viruses, yeast, etc.), physical (laser ablation, arc 23 discharge, photolithography, ball milling, etc.), chemical (Salvo-thermal, sol-gel, co-precipitation, pyrolysis, etc.), technique [8]. Many times, toxic chemicals and solvents are used in physical and chemical processes which could hurt the environment [9]. Within the several synthetic techniques for silver nanoparticles. Biological methods seem to be simple, efficient, and harmless. For translational studies, reliable and environmentally friendly methods that can produce well-defined sizes and shapes are best. Finally, a green chemical approach for the synthesis of AgNPs is quite promising [5]. In the fields of antifungal, antibacterial, cosmetics, anti-inflammatory, antiviral, anticancer, and more green-produced AgNPs have a wide range of uses [10,11]. In reality, plant metabolites have a more well-known intrinsic potential than microorganisms to act as reducing and capping agents and contribute to the aggregation of metal ions into nanoparticles. Reduced Ag has been linked to several biological processes in microorganisms, including optimal development and function as well as cell membrane structure. This is due to interactions between the released Ag ions and macromolecules in these cells, such as proteins and deoxyribonucleic acid (DNA) [12,13]. Additionally, the application of green synthesis aids in the valorization of medicinal plants historically utilized in underdeveloped countries, as stated in the "Traditional Medicinal Strategy" proposed by the World Health Organization (2013) [14].

A topic of current interest is the investigation of a few native plants that assisted in the synthesis of AgNPs. Therefore, this study mainly focused on undertaking the plant-mediated synthesis of silver nanoparticles utilizing *Rhus chinensis* root and leaf extracts in an eco-friendly, cost-effective, and more efficient manner with its antimicrobial application. To the best of our knowledge and many more literature surveys, the green synthesis of silver nanoparticles using aqueous root and leaf extracts of *Rhus chinensis* Mill along with its antimicrobial application have not been well reported yet. Therefore, to overcome these gaps the prepared silver nanoparticles (AgNPs) were characterized by Ultraviolet–visible spectroscopy (UV–Vis), Fourier transform infrared (FTIR), X-ray diffraction spectroscopy (XRD), field emission-scanning electron microscopy (FE-SEM), and energy dispersive X-ray (EDX). The present study also focused on the evaluation of the antibacterial activity of plant-assisted synthesized silver nanoparticles using different parts of *Rhus chinensis* Mill.

2. Materials and methods

2.1. Materials

Plant materials were thoroughly washed with clean water cut into smaller pieces dried in shade for two weeks and then ground into a powder form. Deionized water was used throughout the experiment. Analytical grade silver nitrate was purchased from Thermo Fisher Scientific India Pvt. Ltd.; neomycin, Muller Hinton Agar (MHA), Muller Hinton Broth (MHB) of Himedia Pvt. Ltd. India *Staphylococcus aureus* ATCC 43300, and *Klebsiella pneumonia* ATCC 700603 strains were sourced from the American Type Culture Collection (ATCC).

2.2. Methods

2.2.1. Plant collection and identification

The *Rhus chinensis* plant was harvested in the Arghakhanchi district of western Nepal, at an altitude of 2515 m with a latitude 28′45″ N and longitude of 83′23″ E and its various parts, including leaves, fruits, barks, and roots, were collected in their wild and natural habitat. The plant was identified by the local people as a medicinally important plant. The plant was collected in June and July 2022. After the collection, its herbarium was prepared for its identification by a taxonomist of Godawari Lalitpur's National Herbarium and Plant Laboratories Nepal as *Rhus chinensis* Mill of family Anacardiaceae with voucher code no. MB-OO1 (KATH).

2.2.2. Preparation of plant extracts and silver nanoparticles

2.2.2.1. Plant extracts. Firstly 5 g of fine powder *Rhus chinensis* roots and leaves were well mixed with 100 mL deionized water in a conical flask before boiling at 60 °C for 30 min while being constantly stirred by a heating magnetic stirrer (Nike). The resultant combination was filtered and cooled [15]. Aqueous extracts were stored at 4 °C for the extracts-assisted/green synthesis of silver nanoparticles.

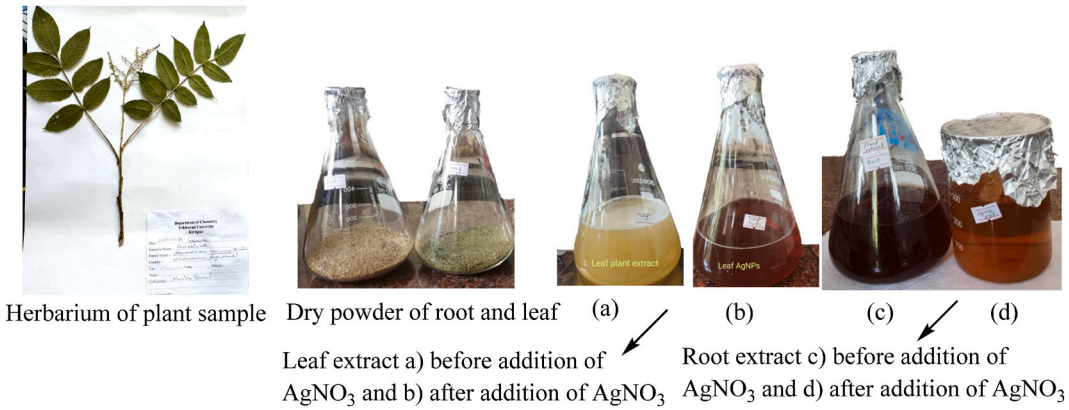

Fig. 1. Plant sample, powder form of sample, visible observation of color change of plant extract before and after the addition of silver nitrate.

2.2.2.2. Synthesis of silver nanoparticles. Different concentrations of the plant extract were allowed to react with the 1 mM silver nitrate solution in the ratios: 1:10, 1:9, 1:8, 1: 5, 1:4, and 1:1. After being stirred for 20 min using a magnetic stirrer, the solution was stored in the dark. The color change from pale yellow to reddish-brown provided preliminary evidence that silver nanoparticles had formed. In the UV–visible range of 300–600 nm, the UV spectra were recorded at three time intervals, namely 0 h, 24 h, and 72 h to check the stability of silver nanoparticles [16]. The optimal ratio of plant extract to 1 mM silver nitrate solution and the best time for nanoparticle production was calculated to be a 1:10 ratio for the leaf extract whereas a 1:4 ratio for the root extract with a reaction duration of 24 h. Then, the reaction mixture (plant extracts + silver nitrate solution) was centrifuged (Sorvall ST 8R) at 8000 rpm for 30 min. Thus, collected silver nanoparticles were stored in a refrigerator at 4 °C to prevent the sample from agglomeration. The plant samples collected, the sample prepared, and the color changed after the addition of $AgNO_3$ are shown in Fig. 1.

2.2.3. Characterization of silver nanoparticles

The characterization of silver nanoparticles was performed to examine the size, shape, element constituents, color mapping, functional group, crystallinity, and quantity of the particles. The preliminary check for the formation of silver nanoparticles was carried out UV–visible spectrophotometer [SPECORD 200 PLUS, (An Endress + Hauser Company)]. The absorption spectra of the samples were examined at wavelengths between 300 and 600 nm using deionized water as a reference solvent to adjust the baseline [17]. The absorption peak confirmed the formation of silver nanoparticles.

Utilizing FTIR analysis (Shimadzu IR Tracer100), the functional groups of organic compounds on the surface of the silver nanoparticles, as well as plant extract, were identified, and the spectra were scanned in the range of 400–4000 cm^{-1} in which the data were plotted using Origin 2019b (9.65) software. Freeze-dried fine powder of AgNPs was employed for XRD analysis utilizing an X-ray diffractometer (D2phaser Bruker, NAST, Nepal) in wavelength 1.540 Å and 30 KV to confirm the crystal structure of AgNPs. The working conditions were typically 2θ scanning between 10° and 20° and all the data obtained were analyzed by using Origin 2019b (9.65) software. To calculate the size of the crystalline silver nanoparticles Scherer's equation was used.

The magnified images of the size, shape, composition, crystallography, and other physical and chemical properties of the specimen were determined by using Field emission-scanning electron microscopy (SU-70 instrument, Korea) [5]. The particle size of silver nanoparticles was measured with the help of ImageJ software from FE-SEM images. The EDX images were recorded at accelerating 10 eV along with at 20000 magnifications.

2.2.4. Antimicrobial activity

Gram-positive *Staphylococcus aureus* ATCC 43300 and Gram-negative *Klebsiella pneumoniae* ATCC 700603 were used as test pathogens to evaluate the antimicrobial activity of silver nanoparticles.

The disc-diffusion method was used to determine the antimicrobial activity of silver nanoparticles [18]. To protect people from various infections, it is necessary to design and create bactericidal and fungicidal agents. Good antibacterial abilities are provided by silver nanoparticles (AgNPs) [19]. The root and leaf extracts assisted synthesized powdered form silver nanoparticles were dissolved in distilled water of concentration 50 μg/mL and left for sonication until it was fully dissolved. 20 μL of silver nanoparticles stock solution was introduced on the Whatmann's filter paper discs of 6 mm to make paper discs and then dried for 10 min 1 mg/mL of neomycin and distilled water were used as a positive and negative control. Using a sterile cotton swab, bacterial culture taken from the suitable inoculums was uniformly distributed over the Petri plates containing Muller- Hilton bacteria to assess the antimicrobial activity of plant extract and extracts assisted synthesized silver nanoparticles. Then, both plant extract and synthesized silver nanoparticles were put on the outer layer of the plates and cultured for a day at the temperature of 37 °C. A scale ruler was used to calculate the ZOI. The experiment was performed in triplicate, and the results were reported as mean ± standard deviation.

2.2.5. Statistical analysis

All the experimental data were performed in triplicate and the results were expressed as the mean ± SD. The data were analyzed by

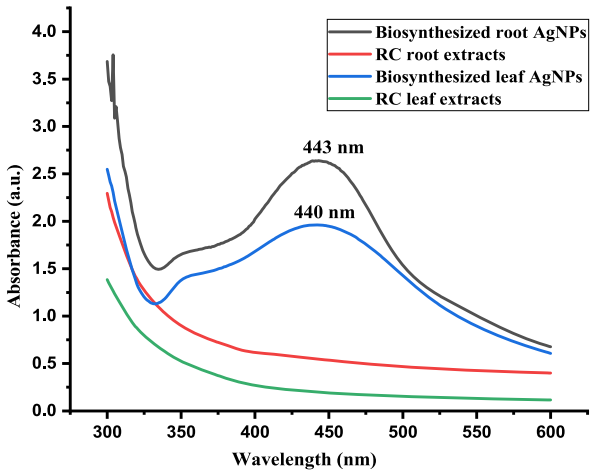

Fig. 2. UV–visible spectral analysis of the root and leaf extracts assisted silver nanoparticles.

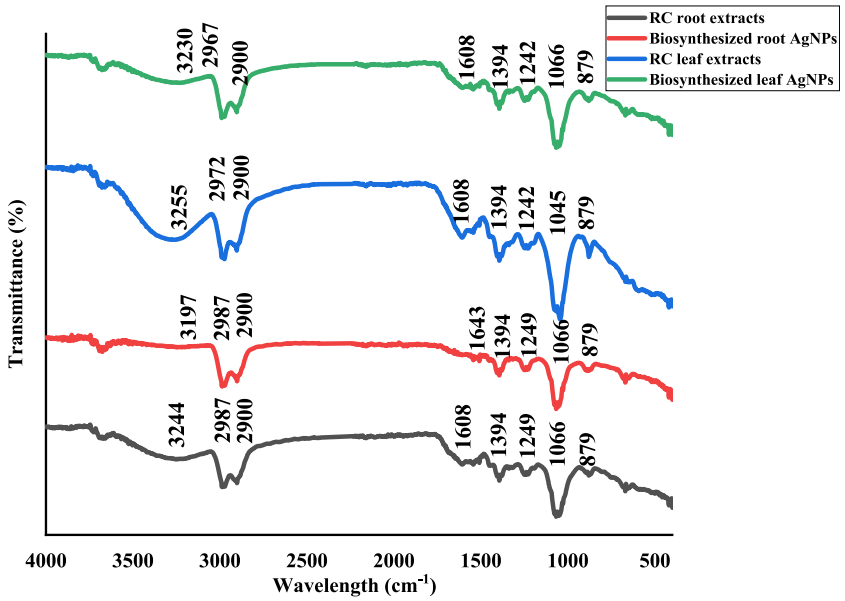

Fig. 3. FTIR spectrum of root and leaf extracts assisted synthesized AgNPs.

using Origin 2019b (9.65) software.

3. Results and discussion

3.1. Visual observation and UV–vis spectroscopy

Spectral analysis was performed after visual confirmation by seeing a color shift during the root and leaf extracts-assisted synthesis of AgNPs which showed a similar pattern to the previously reported results [20]. The yellowish-green color of the reaction mixture shifted to brown (Fig. 1), indicating the transformation of ionic silver (Ag^{+}) into metallic silver (Ag◦), which self-assembles into colloidal particles (AgNPs) supported by the literature [21]. Certain plant secondary metabolites in the extracts have a reducing character and cause silver ions to be reduced to metallic silver [22]. After the addition of $AgNO_3$ solution to the root and leaf extracts the UV–visible spectroscopy shows the absorption in the range of 300–600 nm. The biosynthesized AgNPs of the RC-root sample showed the maximum absorption peak at wavelength 443 nm whereas leaf extract-assisted synthesized AgNPs showed the maximum absorption at wavelength 440 nm respectively in which almost the same results were reported by [23]. The presence of AgNPs is confirmed by the UV–vis bands that were seen, which was caused by SPR absorption [24]. Nanoparticles typically exhibit surface plasmon resonance as a result of the excitation of the free electrons. At 0 h and 24 h, it was found to be the most effective period for the

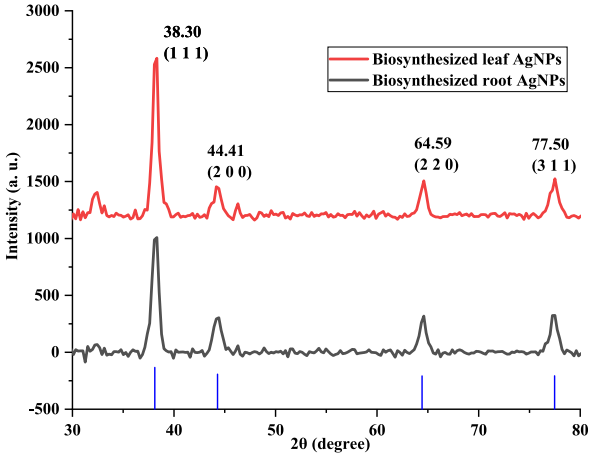

Fig. 4. XRD pattern of synthesized AgNPs assisted by root and leaf extracts of *R. chinensis* along with JCPDS-ICDD files no. 00-004-0783.

creation of stable silver nanoparticles. A UV–visible spectral analysis of the biosynthesized silver nanoparticles of *Rhus chinensis* root and leaf is shown in Fig. 2. This is the first report on the synthesis of silver nanoparticles using an aqueous extract of the root and leaf of *Rhus chinensis* Mill but its gall part has already been used in the synthesis of nanoparticles [25].

3.1.1. Fourier transform infrared spectroscopy (FTIR)

Comparative FTIR spectra were taken for both the plant extracts and plant extracts-assisted AgNPs, respectively. The shifting of signals as a peak helps in the identification of functional groups, and bonding information of biomolecules specifically on the synthetic AgNPs, and the plant extracts. FTIR measurements of both the aqueous root and leaf extracts and the extracts-assisted synthesized nanoparticles were carried out to identify the possible biomolecules responsible for the reduction of the Ag^{+} ions and capping of the bio-reduced silver nanoparticles synthesized assisted by root and leaf extract [26]. The FTIR spectra of plant extracts and the extracts-assisted synthesized AgNPs are shown in Fig. 3.

The transmission peaks at 3244, 2987, 2900, 1608, 1394, 1249, 1066, 879, and 670 cm^{-1} for the root extract, whereas, the transmission peaks at 3197, 2987, 2900, 1543, 1394, 1249, 1066, 870, and 669 cm^{-1} for AgNPs assisted by root extract of *R. chinensis*. Similarly, the peaks appear at 3255, 2972, 2900, 1608, 1394, 1242, 1045, and 879 cm^{-1} are of leaf extract whereas, peaks at 3230, 2987, 2900, 1608, 1394 1242, 1066,179, and 669 cm^{-1} are appeared due to the AgNPs synthesized by using the leaf extract. From these results, the broad and strong absorption band in the region of 3244 cm^{-1} in root extract and 3255 cm^{-1} for leaf extract shifted to 3197 cm^{-1} in the root extract assisted synthesized AgNPs whereas 3230 cm^{-1} in the leaf extract assisted synthesized AgNPs. This is due to the stretching frequency of a polyphenolic –OH group present in the plant extracts [27]. The band in FT-IR at 1608 cm^{-1} is due to the C═C stretch of alkenes or the C═O stretch of amides. The transformation in wavelength from 1608 to 1543 cm^{-1} indicates the attachment of the (N–H) CO group to the nanoparticles. The aromatic C–H stretching band is assigned at 2987-2972 cm^{-1}. The peak at 1394 cm^{-1} is attributed to C–N stretching, due to the presence of an aliphatic amine group in the protein. Absorption at 650–880 cm^{-1} is brought on by = CH in aromatic compounds. The absorption bands at 1020–1250 cm^{-1}, show the carbon-carbon stretching in an organic compound found in plant extracts. It has been reported that the involvement of functional groups like N–H, C═O, and C–C while synthesizing the plant extracts assisted AgNPs [25]. These results showed that oxidized polyphenols have capped the surface of AgNPs. The findings of this study are some comparable and consistent with the previously reported results in the plant mediated synthesis of nanoparticles [28].

3.1.2. X-ray diffraction (XRD)

The X-ray diffraction study was carried out to establish the crystalline nature of the particles. The XRD pattern of synthesized AgNPs assisted by root extracts has shown four intense peaks corresponding to (111), (200), (220), and (311) planes of the face-centered cubic lattice structure of metallic silver (JCPDS-ICDD files no. 00-004-0783, which verifies the crystalline character of silver nanoparticles and validates their effective synthesis [29]. Bragg's reflection ($2\theta = 38.30°$, 44.41°, 64.59°, and 77.50°). Similarly, AgNPs synthesized by assisting the root extract have shown four intense peaks corresponding to (111), (200), (220), and (311). Bragg's reflection ($2\theta =$ 38.30°, 44.41°, 64.59°, and 77.50°) is due to the structure of AgNPs. The average crystallite size of the root extract-assisted synthesized AgNPs was calculated using the Debye-Scherer formula to determine the width of each diffraction peak after the Gaussian fitting of all four peaks and found as 11.01 nm and 13.39 nm respectively. The size of nanoparticles reported in the literature was less than the size found in this study [30], the crystallite size of silver nanoparticles was found to be 5 nm. The XRD patterns of AgNPs are shown in Fig. 4.

3.1.3. Field emission scanning electron microscopy (FE-SEM)

The FE-SEM was used to analyze the morphological structure as well as to calculate the particle size of nanoparticles. High-density

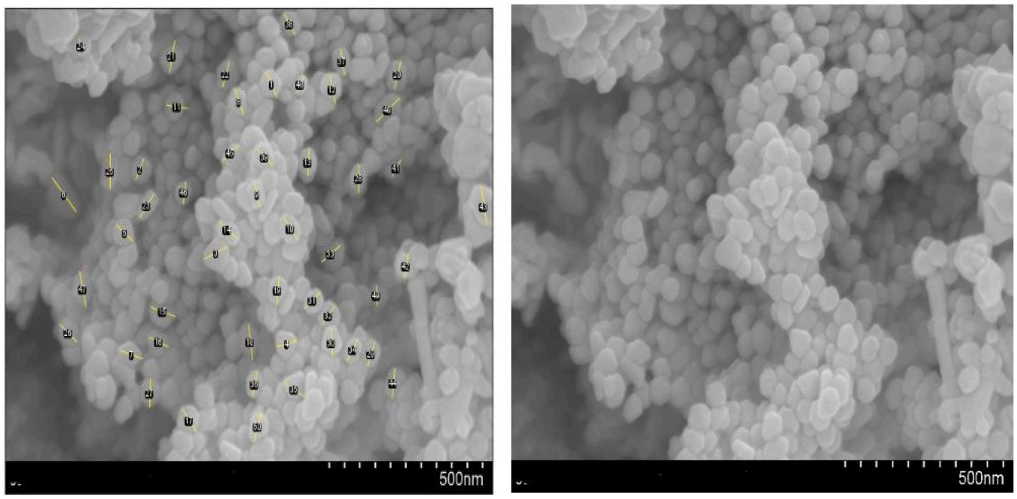

(a) Calculated particle size FE-SEM images at a resolution of 500 nm

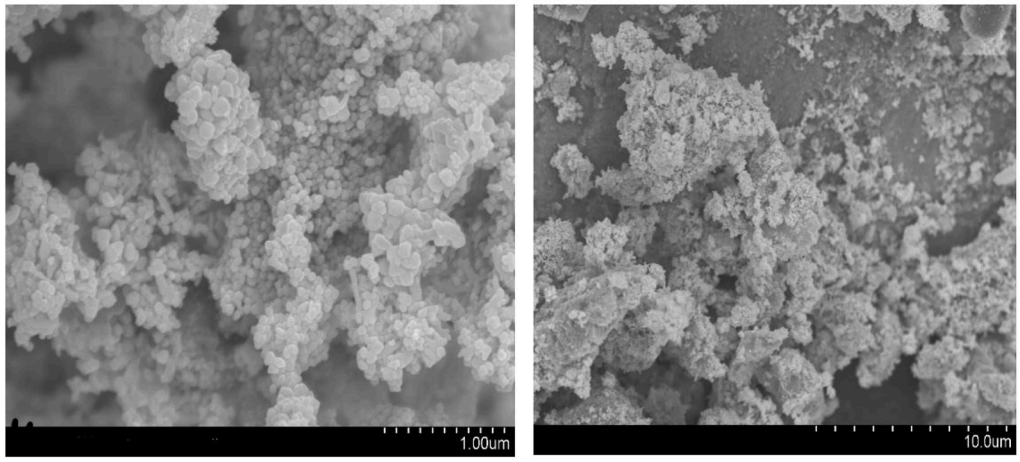

(b) FE-SEM images at a resolution of 1.0 μm

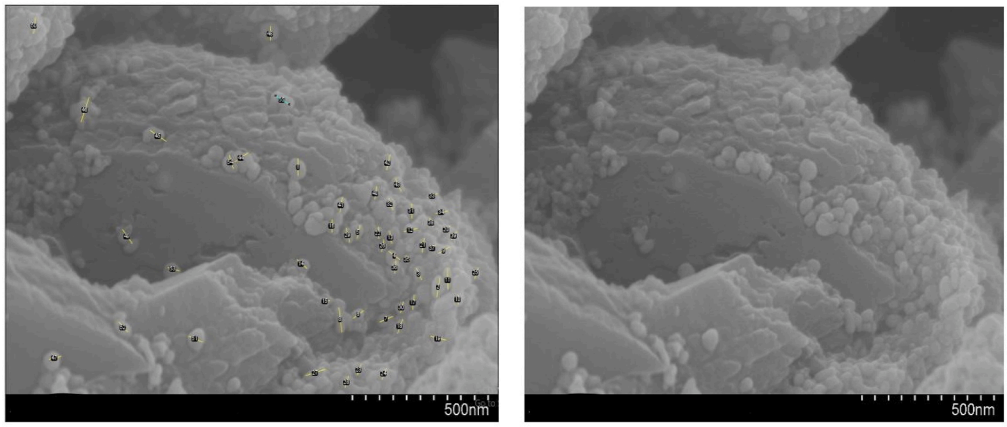

(c) FE-SEM images at a resolution of 10.0 μm

Fig. 5. FE-SEM images of synthesized AgNPs using root extract.

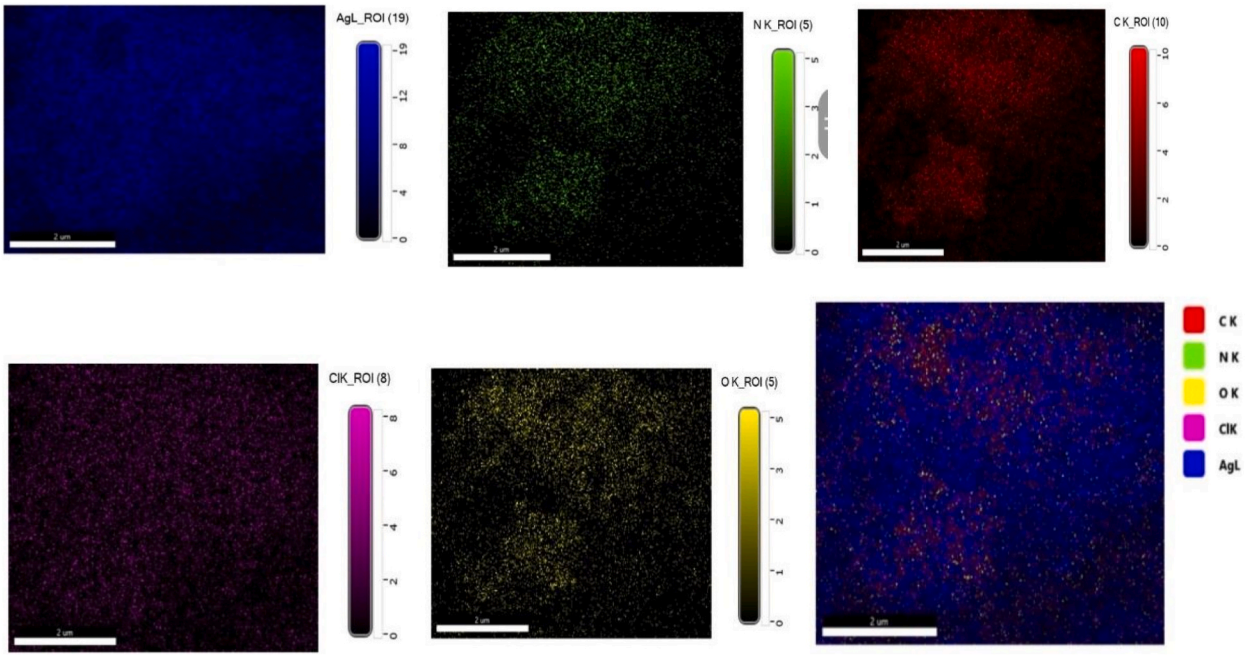

Fig. 6. An energy-dispersive x-ray (EDX) spectrum of AgNPs with total elemental mapping and individual color mapping of synthesized AgNPs assisted by root extract.

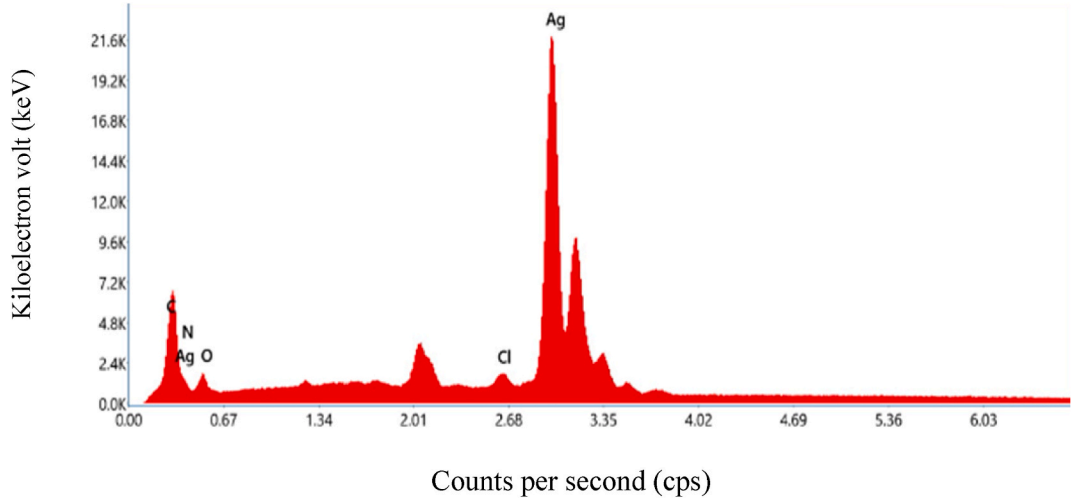

Fig. 7. EDX spectrum of synthesized AgNPs assisted by root extract.

AgNPs were produced by *Rhus chinensis* root and leaf extract, according to FE-SEM examination. It was demonstrated that root extract and leaf extract assisted synthesis of AgNPs were mostly spherical with diameters of 54.40 nm and 30.89 nm, respectively [31]. also examined that synthesized silver nanoparticles formed by using the *Rivina humilis* leaf extract were found to be spherical with a diameter of 51 nm showing some similarity to the present study. The bioorganic capping molecules that were coupled to the silver nanoparticles interacted with one another via hydrogen bonds and electrostatic interactions to produce the silver nanoparticles' SEM image. The FE-SEM images show the particle size at different resolutions which are shown in Fig. 5 (a), (b), and (c) and 8 (a), (b) and (c). EDX spectroscopy was used to evaluate the elemental composition on the surface of the biosynthesized nanomaterials. The EDX study and the color map proved the presence of the silver component. Figs. 6 and 9 showed the elemental mapping of synthesized AgNPs revealed the presence of silver, carbon, chlorine, oxygen, and nitrogen. Through, EDX the peak of silver in both AgNPs assisted by root and leaf extracts showed around 3 Kev due to SPR [32] and other elements like Cl, O, C, and N were also reported in synthesized AgNPs which were matched to the results reported in the literature [25]. Since, plant secondary metabolites serve as both capping and reducing agents in the extracts-assisted synthesis of AgNPs [33]. The FE-SEM of root extract-assisted synthesized AgNPs is shown in

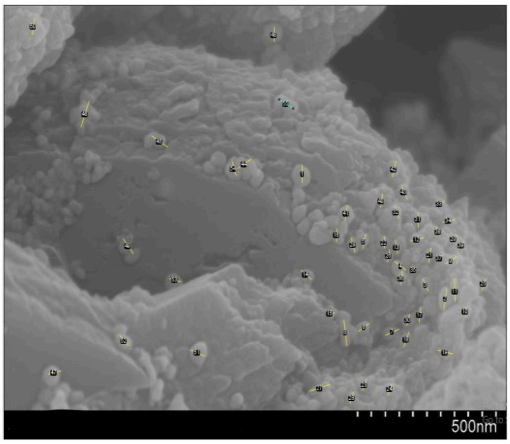

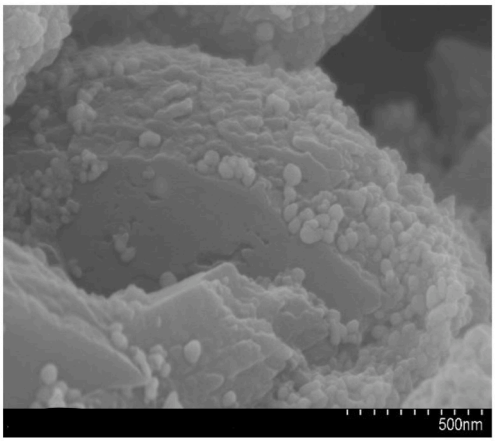

(a) Calculated particle size FE-SEM images at a resolution of 500 nm

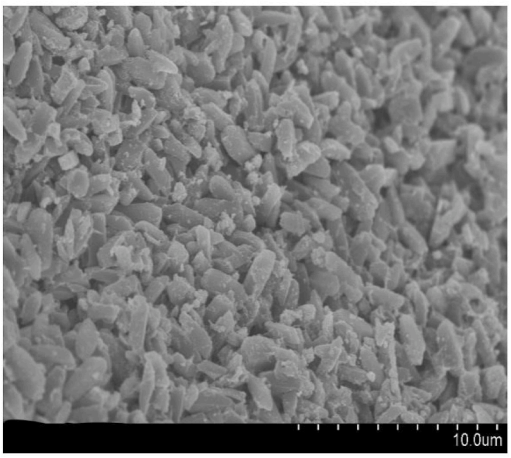

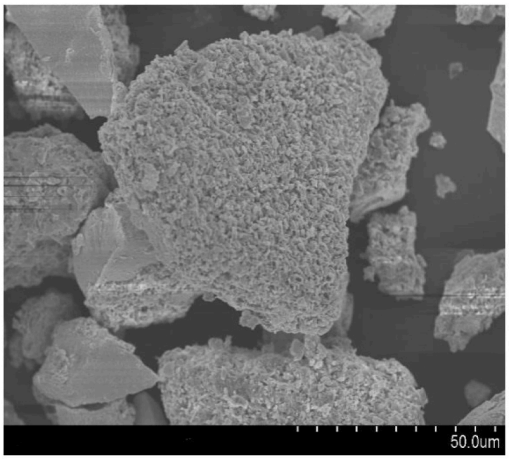

(b) FE-SEM images at a resolution of 10.0 μm. (c) FE-SEM images at a resolution of 50.0 μm

Fig. 8. FE-SEM images of synthesized AgNPs assisted by leaf extract.

Fig. 5. The energy-dispersive X-ray EDX spectrum and elemental mapping of root extract-assisted AgNPs are shown in Fig. 6. The EDX spectrum of root-assisted synthesized AgNPs is shown in Fig. 7. The FE-SEM image of synthesized nanoparticles assisted by leaf extract and energy-dispersive X-ray is shown in Figs. 8 and 10. The particle size distribution is displayed in histograms which is shown in Fig. 11.

3.2. Antimicrobial activity

The disc-diffusion method was used to perform the antibacterial activity shown by root and leaf aqueous extracts and the synthesized silver nanoparticles assisted by the root and leaf extracts. In such a study 1 mg/mL neomycin and distilled water were used as a positive and negative control. The results of anti-bacterial screening are shown in Table 1. The results of antibacterial activity exhibited by the root and leaf extracts assisted AgNPs are displayed in bar diagrams to compare their activity against the bacterial strains used in the study Fig. 12.

Where R = *Rhus chinensis*, L = leaf, R = root A = aqueous S = silver nanoparticles.

From Table 1, the obtained data showed that the root and leaf extract-assisted silver nanoparticles were found active against *Staphylococcus aureus* and *Klebsiella pneumoniae* as compared to the crude aqueous root and leaf extract. Among them, the root-assisted synthesized silver nanoparticle was found active against Gram-positive bacteria *Staphylococcus aureus* showing ZOI 7.83 ± 0.17 mm whereas the leaf-assisted synthesized silver nanoparticles were found active against Gram-negative bacteria *Klebsiella pneumoniae* of ZOI 7.0 ± 0.29 mm. Figs. 13 and 14.

There are several explanations related to the mechanism of antibacterial activity but the actual way of representing mechanism but the actual way of describing is still unknown. The biological activity imparted by the nanoparticles is due to their size and morphology.

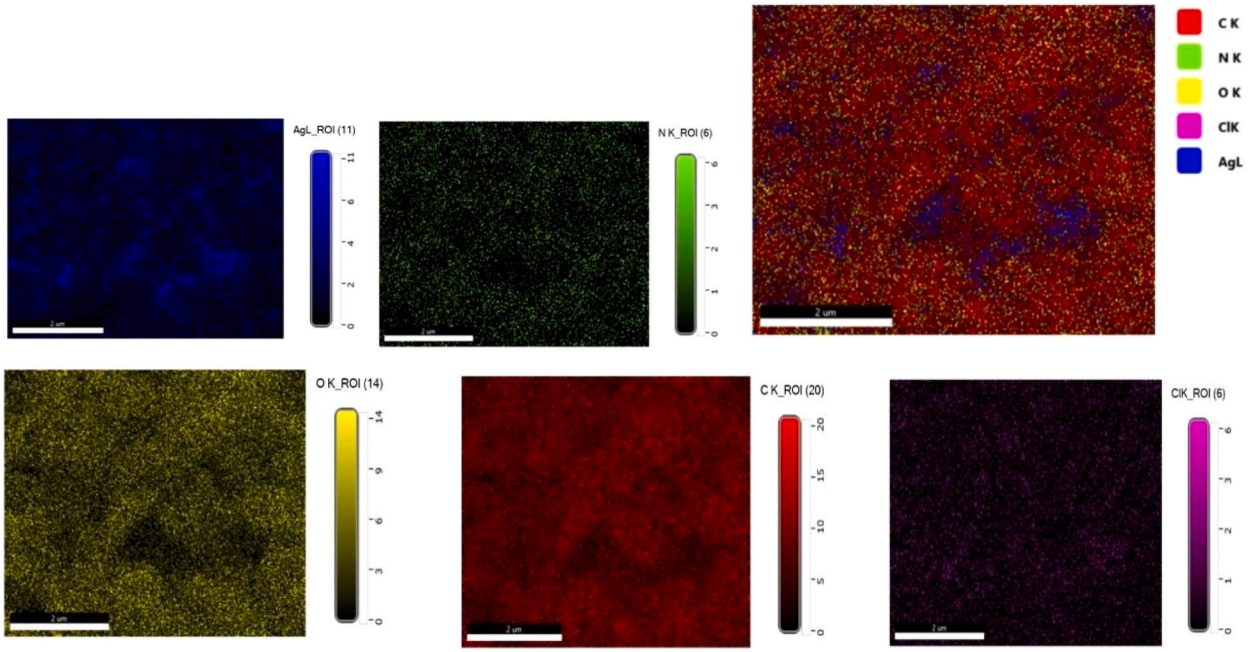

Fig. 9. An energy-dispersive x-ray (EDX) spectrum of AgNPs with total elemental mapping and individual color mapping of AgNPs assisted to be synthesized by leaf extract.

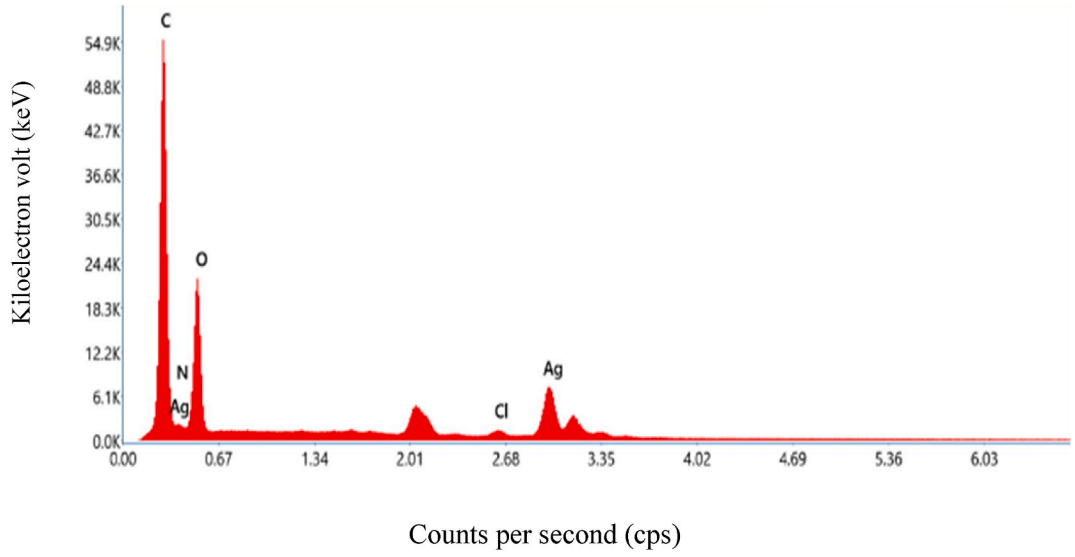

Fig. 10. EDX spectrum of synthesized AgNPs assisted by leaf extract.

Bacterial infections and resistance to antibiotic drugs are the major challenges that threaten the health of humans and animals in different societies of the world. The antibacterial drug seems to be less effective or even ineffective due to this problem of resistance. Several modifications can be made to the structure and composition of the compounds to restore the antimicrobial activity. Many phytochemicals derived from the plant sources have exhibited potent activities against the bacterial resistance. Now modern research focused on the structure-activity relationship and mechanism of action in bacterial cells due to the plant-assisted synthesized nanoparticles can be explained in different ways. Such mechanism is based on the effect on bacterial protein biosynthesis, cell wall biosynthesis, cell membrane disruption, bacterial DNA replication, and repair and inhibition of metabolic pathways. The mechanism of action shown by the plant-assisted synthesized nanoparticles is shown in Fig. 15 (Khameneh et al., 2019).[34].

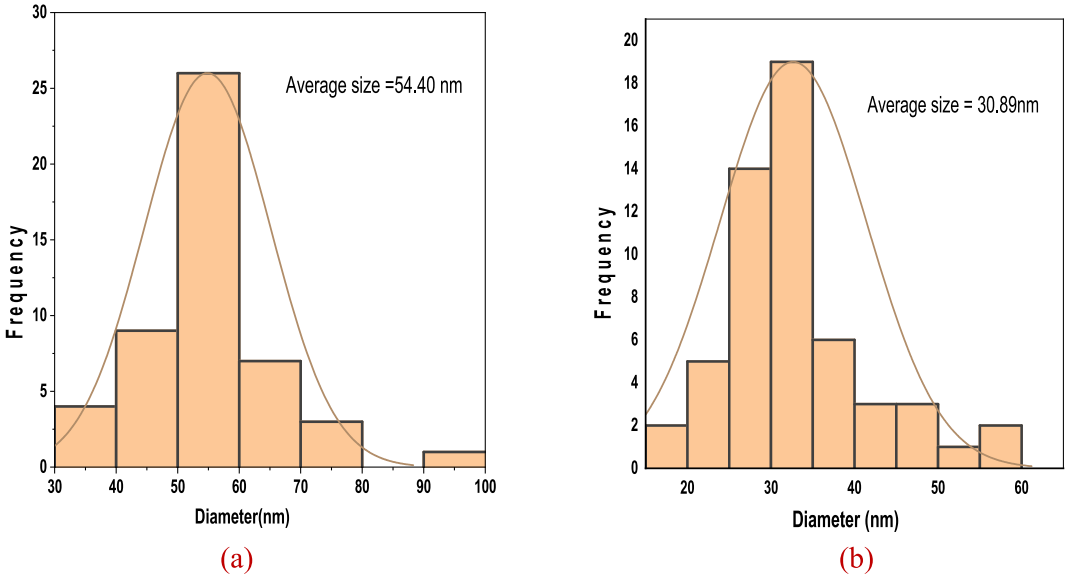

Fig. 11. FE-SEM images of the AgNPs assisted by the (a) root and (b) leaf extracts showing particle size distribution through a histogram.

Table 1
Antimicrobial screening of plant extracts and root and leaf extracts assisted synthesized silver nanoparticles against *Staphylococcus aureus* and *Klebsiella pneumoniae*.

Extracts	Bacteria	ZOI sample (mm)	ZOI positive control (neomycin)
RC- leaf aqueous	*Staphylococcus aureus* ATCC	7.0 ± 0.0	18
RC-leaf AgNPs	43300	7.5 ± 0.29	17
RC- root aqueous		6.0 ± 0.0	18
RC- root AgNPs		7.83 ± 0.17	17
RC- leaf aqueous	*Klebsiella pneumoniae* ATCC 700603	5.67 ± 0.17	20
RC-leaf AgNPs		7.0	20
RC- root aqueous		5.0 ± 0.0	17
RC- root AgNPs		6.17 ± 0.17	20

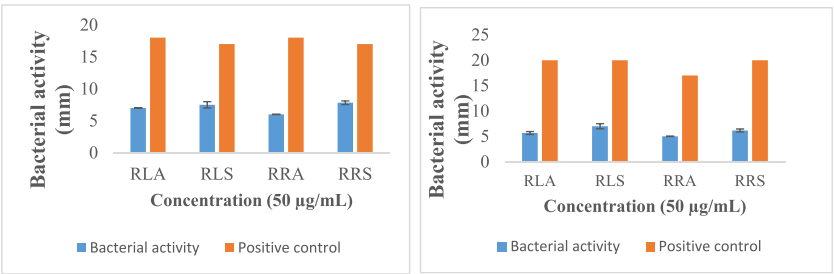

Fig. 12. Antibacterial activity (ZOI in mm) was shown by plant extract and silver nanoparticles against (a) *Staphylococcus aureus* and (b) *Klebsiella pneumoniae.*

4. Conclusions

Plant extracts-assisted synthesis of silver nanoparticles is a quicker, more efficient, and less expensive method. Since the synthesis doesn't result in the creation of any hazardous chemicals. It has been demonstrated that an extract of the leaf and root of *R. chinensis* acts as a good reductant for the manufacture of colloidal silver nanoparticles. UV–visible spectroscopy confirmed the formation of silver nanoparticles in an aqueous medium, XRD determined the crystallite nature of silver nanoparticles based on the face-centered cubic structure of silver nanocrystal. FTIR verified the formation of silver nanoparticles utilizing phytoconstituents, correlating to the reducing and stabilizing agents in chemical synthesis. Similarly, FE-SEM analyses verified the formation of spherical-shaped silver

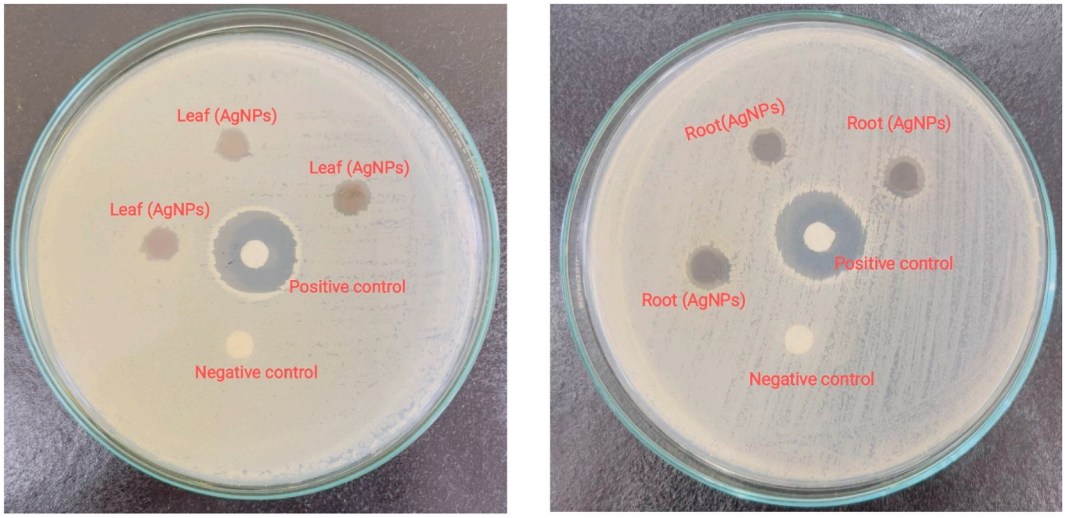

Fig. 13. The antibacterial activity showed by (a) leaf extract-assisted synthesized AgNPs and (b) root extract-assisted synthesized AgNPs against *Staphylococcus aureus*.

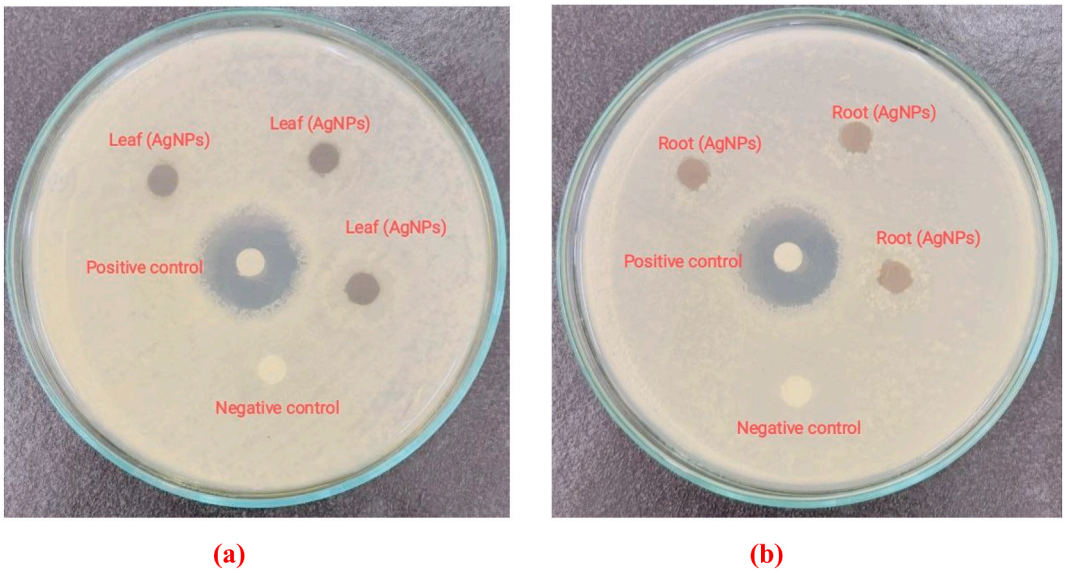

Fig. 14. The antibacterial activity was shown by (a) leaf extracts-assisted synthesized AgNPs and (b) root extract-assisted synthesized AgNPs against *Klebsiella pneumoniae*.

nanoparticles, and the presence of silver components was proved through EDX. On the other hand, the greenly synthesized silver nanoparticles assisted by the root and leaf extracts of *Rhus chinensis*, demonstrated their antibacterial effectiveness against several microbes. In contrast, the silver nanoparticles made by using the root extract demonstrated effective suppression of bacterial activity. As a result, it is concluded that the root and leaf of *Rhus chinensis* Mill might be a source for the isolation and characterization of capping, reducing, and stabilizing agents for synthesizing the silver nanoparticles as the natural origin. To address advanced potential future issues, more research should be done on the pharmacological properties of *Rhus chinensis* Mill and the plant-assisted nanoparticles.

Funding statement

This research was partially supported by the Nepal Academy of Science and Technology (NAST), of grant no. 35/2080/81.

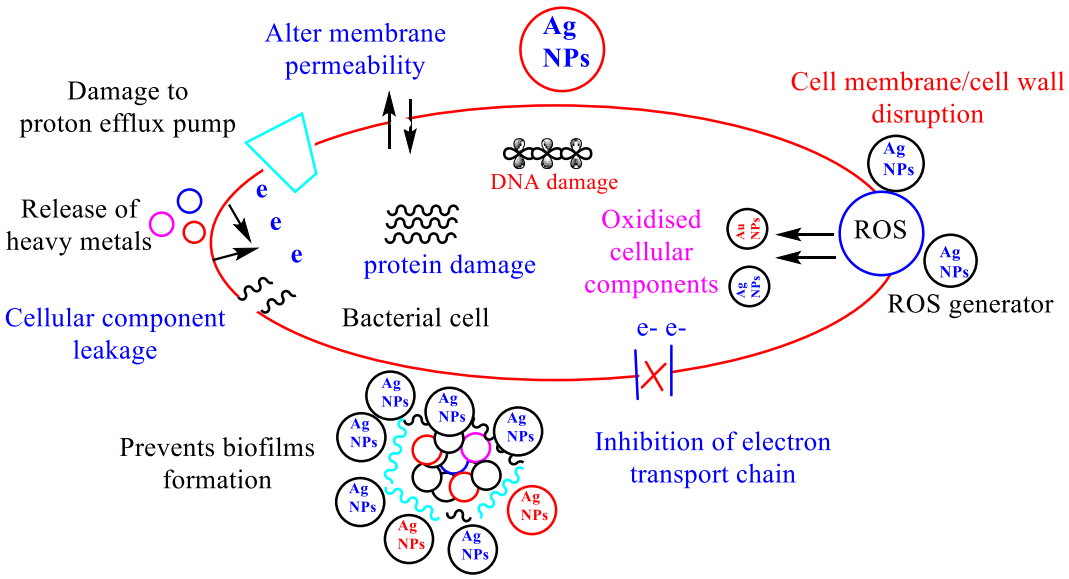

Fig. 15. Mechanism of antibacterial activity shown by AgNPs.

Additional information

No additional information is available for this paper.

Data availability statement

All the data generated in this study will be provided on request. The data are uploaded into the wave link of the journal while submitting the paper.

CRediT authorship contribution statement

Manisha Bhusal: Writing – review & editing, Writing – original draft, Methodology, Formal analysis. **Ishwor Pathak:** Writing – review & editing, Data curation. **Anita Bhadel:** Writing – review & editing, Visualization, Data curation. **Deepak Kumar Shrestha:** Writing – review & editing, Data curation. **Khaga Raj Sharma:** Writing – review & editing, Supervision, Conceptualization.

Declaration of competing interest

The authors declare the following financial interests/personal relationships which may be considered as potential competing interests:Manisha Bhusal reports financial support was provided by Nepal Academy of Science and Technology. If there are other authors, they declare that they have no known competing financial interests or personal relationships that could have appeared to influence the work reported in this paper.

Acknowledgments

National Herbarium and Plant Laboratories, Godawari, Nepal is thankful for the identification of the plant. We are thankful to the Nepal Academy of Science and Technology (NAST) for providing partial financial support to the first author Manisha Bhusal.

Appendix A. Supplementary data

Supplementary data to this article can be found online at https://doi.org/10.1016/j.heliyon.2024.e33603.

References

[1] D. Odilon, W. Yao, Rhus chinensis and galla chinensis - folklore to modern evidence: review, Phytother Res. : PTR 24 (2010) 1739–1747, https://doi.org/10.1002/ptr.3215.

[2] R.-R. Wang, Q. Gu, L.-M. Yang, J.-J. Chen, S.-Y. Li, Y.-T. Zheng, Anti-HIV-1 activities of extracts from the medicinal plant *Rhus chinensis*, J. Ethnopharmacol. 105 (1) (2006) 269–273, https://doi.org/10.1016/j.jep.2005.11.008.

[3] T. Klaus, R. Joerger, E. Olsson, C.G. Granqvist, Silver-based crystalline nanoparticles, microbially fabricated, Proc. Natl. Acad. Sci. U.S.A. 96 (24) (1999) 13611–13614, https://doi.org/10.1073/pnas.96.24.13611.

[4] S. Chernousova, M. Epple, Silver as antibacterial agent: ion, nanoparticle, and metal, Angew. Chem. Int. Ed. 52 (6) (2013) 1636–1653, https://doi.org/10.1002/anie.201205923.

[5] X.-F. Zhang, Z.-G. Liu, W. Shen, S. Gurunathan, Silver nanoparticles: synthesis, characterization, properties, applications, and therapeutic approaches, Int. J. Mol. Sci. 17 (9) (2016) 1534, https://doi.org/10.3390/ijms17091534.

[6] W.-R. Li, X.-B. Xie, Q.-S. Shi, H.-Y. Zeng, Y.-S. Ou-Yang, Y.-B. Chen, Antibacterial activity and mechanism of silver nanoparticles on Escherichia coli, Appl. Microbiol. Biotechnol. 85 (4) (2010) 1115–1122, https://doi.org/10.1007/s00253-009-2159-5.

[7] M. Sharifi-Rad, H.S. Elshafie, P. Pohl, Green synthesis of silver nanoparticles (AgNPs) by *Lallemantia royleana* leaf Extract: their Bio-Pharmaceutical and catalytic properties, J. Photochem. Photobiol. Chem. 448 (2024) 115318, https://doi.org/10.1016/j.jphotochem.2023.115318.

[8] S.U. Khan, T.A. Saleh, A. Wahab, M.H.U. Khan, D. Khan, W.U. Khan, A. Rahim, S. Kamal, F.U. Khan, S. Fahad, Nanosilver: new ageless and versatile biomedical therapeutic scaffold, Int. J. Nanomed. 13 (2018) 733–762, https://doi.org/10.2147/IJN.S153167.

[9] S. Ahmad, S. Munir, N. Zeb, A. Ullah, B. Khan, J. Ali, M. Bilal, M. Omer, M. Alamzeb, S.M. Salman, S. Ali, Green nanotechnology: a review on green synthesis of silver nanoparticles - an eco-friendly approach, Int. J. Nanomed. 14 (2019) 5087–5107, https://doi.org/10.2147/IJN.S200254.

[10] H.A. Hussein, M.A. Abdullah, Biosynthesis, mechanisms, and biomedical applications of silver nanoparticles, in: D. Thangadurai, J. Sangeetha, R. Prasad (Eds.), Functional Bionanomaterials: from Biomolecules to Nanoparticles, Springer International Publishing, 2020, pp. 313–332, https://doi.org/10.1007/978-3-030-41464-1_14.

[11] S.A. Khan, S. Shahid, B. Shahid, U. Fatima, S.A. Abbasi, Green synthesis of MnO nanoparticles using abutilon indicum leaf extract for biological, photocatalytic, and adsorption activities, Biomolecules 10 (5) (2020) 785, https://doi.org/10.3390/biom10050785.

[12] M. Sharifi-Rad, P. Pohl, F. Epifano, J.M. Álvarez-Suarez, Green synthesis of silver nanoparticles using Astragalus tribuloides delile. Root extract: characterization, antioxidant, antibacterial, and anti-inflammatory activities, Nanomaterials 10 (12) (2020), https://doi.org/10.3390/nano10122383. Article 12.

[13] M. Sharifi-Rad, P. Pohl, Synthesis of biogenic silver nanoparticles (AgCl-NPs) using a pulicaria vulgaris gaertn. Aerial Part Extract and their application as antibacterial, antifungal and antioxidant agents, Nanomaterials 10 (4) (2020), https://doi.org/10.3390/nano10040638. Article 4.

[14] E.K. Kambale, C.I. Nkanga, B.P.I. Mutonkole, A.M. Bapolisi, D.O. Tassa, J.M.I. Liesse, R.W. M. Krause, P.B. Memvanga, Green synthesis of antimicrobial silver nanoparticles using aqueous leaf extracts from three Congolese plant species (*Brillantaisia patula, Crossopteryx febrifuga* and *Senna siamea*), Heliyon 6 (8) (2020) e04493. https://doi.org/10.1016/j.heliyon.2020.e04493.

[15] J. Jalab, W. Abdelwahed, A. Kitaz, R. Al-Kayali, Green synthesis of silver nanoparticles using aqueous extract of Acacia cyanophylla and its antibacterial activity, Heliyon 7 (9) (2021) e08033, https://doi.org/10.1016/j.heliyon.2021.e08033.

[16] R. Giri, K. Sharma, Biogenic synthesis of silver nanoparticles using *Terminalia chebula* Retz. Leaf extract and evaluation of biological activities, J. Nepal Chem. Soc. 43 (1) (2022), https://doi.org/10.3126/jncs.v43i1.46957. Article 1.

[17] K. Anandalakshmi, J. Venugobal, V. Ramasamy, Characterization of silver nanoparticles by green synthesis method using Pedalium murex leaf extract and their antibacterial activity, Appl. Nanosci. 6 (3) (2016) 399–408, https://doi.org/10.1007/s13204-015-0449-z.

[18] K. Khadayat, D.D. Sherpa, K.P. Malla, S. Shrestha, N. Rana, B.P. Marasini, S. Khanal, B. Rayamajhee, B.R. Bhattarai, N. Parajuli, Molecular identification and antimicrobial potential of streptomyces species from Nepalese soil, Int. J. Microbiol. 2020 (2020) 8817467, https://doi.org/10.1155/2020/8817467.

[19] M. Hafeez, M. Zeb, A. Khan, B. Akram, Z.-U. Abdin, S. Haq, M. Zaheer, S. Ali, Populus ciliata mediated synthesis of silver nanoparticles and their antibacterial activity, Microsc. Res. Tech. 84 (3) (2021) 480–488, https://doi.org/10.1002/jemt.23604.

[20] G. Gnanajobitha, K. Paulkumar, M. Vanaja, S. Rajeshkumar, C. Malarkodi, G. Annadurai, C. Kannan, Fruit-mediated synthesis of silver nanoparticles using Vitis vinifera and evaluation of their antimicrobial efficacy, J. Nanostruct. Chem. 3 (1) (2013) 67, https://doi.org/10.1186/2193-8865-3-67.

[21] L.N. Khanal, K.R. Sharma, H. Paudyal, K. Parajuli, B. Dahal, G.C. Ganga, Y.R. Pokharel, S.K. Kalauni, Green synthesis of silver nanoparticles from root extracts of *Rubus ellipticus* Sm. And comparison of antioxidant and antibacterial activity, J. Nanomater. 2022 (2022) e1832587, https://doi.org/10.1155/2022/1832587.

[22] G.Z.S. Oliveira, C.A.P. Lopes, M.H. Sousa, L.P. Silva, Synthesis of silver nanoparticles using aqueous extracts of Pterodon emarginatus leaves collected in the summer and winter seasons, Int. Nano Lett. 9 (2019), https://doi.org/10.1007/s40089-019-0265-7.

[23] S. Periasamy, U. Jegadeesan, K. Sundaramoorthi, T. Rajeswari, V.N.B. Tokala, S. Bhattacharya, S. Muthusamy, M. Sankoh, M.K. Nellore, Comparative analysis of synthesis and characterization of silver nanoparticles extracted using leaf, flower, and bark of Hibiscus rosasinensis and examine its antimicrobicidal activity, J. Nanomater. 2022 (2022) e8123854, https://doi.org/10.1155/2022/8123854.

[24] E.K. Kambale, C.I. Nkanga, B.-P.I. Mutonkole, A.M. Bapolisi, D.O. Tassa, J.-M.I. Liesse, R.W.M. Krause, P.B. Memvanga, Green synthesis of antimicrobial silver nanoparticles using aqueous leaf extracts from three Congolese plant species (*Brillantaisia patula, Crossopteryx febrifuga* and *Senna siamea*), Heliyon 6 (8) (2020) e04493, https://doi.org/10.1016/j.heliyon.2020.e04493.

[25] M.P. Patil, A.A. Rokade, D. Ngabire, G.-D. Kim, Green synthesis of silver nanoparticles using water extract from galls of Rhus chinensis and its antibacterial activity, J. Cluster Sci. 27 (5) (2016) 1737–1750, https://doi.org/10.1007/s10876-016-1037-4.

[26] G. Suresh, P.H. Gunasekar, D. Kokila, D. Prabhu, D. Dinesh, N. Ravichandran, B. Ramesh, A. Koodalingam, G. Vijaiyan Siva, Green synthesis of silver nanoparticles using *Delphinium denudatum* root extract exhibits antibacterial and mosquito larvicidal activities, Spectrochim. Acta Mol. Biomol. Spectrosc. 127 (2014) 61–66, https://doi.org/10.1016/j.saa.2014.02.030.

[27] A. Hussain, A. Mehmood, G. Murtaza, K.S. Ahmad, A. Ulfat, M.F. Khan, T.S. Ullah, Environmentally benevolent synthesis and characterization of silver nanoparticles using *Olea ferruginea* Royle for antibacterial and antioxidant activities, Green Process. Synth. 9 (1) (2020) 451–461, https://doi.org/10.1515/gps-2020-0047.

[28] S. Dangi, A. Gupta, D.K. Gupta, S. Singh, N. Parajuli, Green synthesis of silver nanoparticles using aqueous root extract of Berberis asiatica and evaluation of their antibacterial activity, Chem. Data Collect. 28 (2020) 100411, https://doi.org/10.1016/j.cdc.2020.100411.

[29] V. Dhand, L. Soumya, S. Bharadwaj, S. Chakra, D. Bhatt, B. Sreedhar, Green synthesis of silver nanoparticles using Coffea arabica seed extract and its antibacterial activity, Mater. Sci. Eng., C 58 (2016) 36–43, https://doi.org/10.1016/j.msec.2015.08.018.

[30] L. Karthik, G. Kumar, A.V. Kirthi, A.A. Rahuman, K.V. Bhaskara Rao, Streptomyces sp. LK3 mediated synthesis of silver nanoparticles and its biomedical application, Bioproc. Biosyst. Eng. 37 (2) (2014) 261–267, https://doi.org/10.1007/s00449-013-0994-3.

[31] S. Raghava, K. Munnene Mbae, S. Umesha, Green synthesis of silver nanoparticles by Rivina humilis leaf extract to tackle growth of Brucella species and other perilous pathogens, Saudi J. Biol. Sci. 28 (1) (2021) 495–503, https://doi.org/10.1016/j.sjbs.2020.10.034.

[32] P. Magudapathy, P. Gangopadhyay, B.K. Panigrahi, K.G.M. Nair, S. Dhara, Electrical transport studies of Ag nanoclusters embedded in glass matrix, Phys. B Condens. Matter 299 (1) (2001) 142–146, https://doi.org/10.1016/S0921-4526(00)00580-9.

[33] H. Bagur, C.C. Poojari, G. Melappa, R. Rangappa, N. Chandrasekhar, P. Somu, Biogenically synthesized silver nanoparticles using endophyte fungal extract of *Ocimum tenuiflorum* and evaluation of biomedical properties, J. Cluster Sci. 31 (6) (2020) 1241–1255, https://doi.org/10.1007/s10876-019-01731-4.

[34] B. Khameneh, M. Iranshahy, V. Soheili, B.S. Fazly Bazzaz, Review on plant antimicrobials: A mechanistic viewpoint, Antimicrobial Resistance & Infection Control 8 (1) (2019) 118. https://doi.org/10.1186/s13756-019-0559-6.